

Nickel Sub-lattice Effects on the Optical Properties of ZnO Nanocrystals

Sajid Husain¹, F. Rahman¹, Nasir Ali², P. A. Alvi^{3,*}

¹Department of Physics, Aligarh Muslim University, Aligarh, India

²School of Physical Science, Jawaharlal Nehru University, New Delhi, India

³Department of Physics, Banasthali University, Banasthali Vidyapith, Rajasthan, India

*Corresponding author: drpaalvi@gmail.com

Received November 14, 2013; Revised December 04, 2013; Accepted December 22, 2013

Abstract Nano-crystalline undoped and Ni doped ZnO (Ni-ZnO) nano-particles with compositional formula $\text{Ni}_x\text{Zn}_{1-x}\text{O}$ ($x=0, 1, 3$ and 5 mol %) were synthesized using sol-gel method. As nickel incorporated in to the ZnO matrix results were analyzed using different techniques such as XRD, SEM, EDS, UV-VIS and FT-IR techniques. X-ray diffraction (XRD) result reveals the formation of hexagonal wurtzite structure of all samples, while extra peak appears at 42.5° due to Ni sub-lattice in doped samples informs about the presence of doped species. In addition, the surface morphology of undoped ZnO has also been studied and discussed using scanning electron microscopy (SEM). Moreover, the energy bandgap of undoped and doped ZnO has also been measured using UV-VIS spectrometer. It is observed that the doping of sub-lattice affects the structure as well as the energy bandgap. Hence, by Ni- doping in ZnO nano-particles, the energy bandgap of Ni-ZnO can be tuned for various optical applications. The lattice parameters and crystallite sizes have also been determined using XRD and it has been observed that they changes with the increase of Ni amount. The crystal vibrational study has also been performed using FT-IR spectroscopy which gives the presence of the host as well as doped sub-lattice.

Keywords: Ni-ZnO, nano-particles, sol-gel, XRD, SEM, EDS, FT-IR, UV-VIS

Cite This Article: Sajid Husain, F. Rahman, Nasir Ali, and P. A. Alvi, "Nickel Sub-lattice Effects on the Optical Properties of ZnO Nanocrystals." *Journal of Optoelectronics Engineering* 1, no. 1 (2013): 28-32. doi: 10.12691/joe-1-1-5.

1. Introduction

In last decades or even recent years, doped zinc oxide (ZnO) has been the subject of much attention because of its potential for important applications such as in optoelectronic and luminescent devices [1], heterojunction solar cells [2], and transparent conductors [3] as well as in chemical and gas sensors [4]. It is also an important material for piezoelectric devices [5], surface acoustic waves [6], anti-reflecting coatings [7], etc. This oxide material is of great importance to several applications such as mentioned above and also phototherapy agents, owing to a wide band gap (3.37 eV), large exciton binding energy (60 meV) and semiconductor properties [8]. It is well known that the changes in optical, electrical, and magnetic properties could occur when impurities were added into a wide gap semiconductor, thus doping of a certain amount in to ZnO matrix has become an important route to optimize its optical, electrical, and magnetic performance. It was reported that transition-metal (TM)-doped ZnO would be a good candidate to achieve Curie temperature above the room temperature [9], and great efforts have been devoted to the investigation of magnetic materials [10,11]. Nickel is an important dopant in these magnetic materials. Here, the objective of the study is to

find out the effects of doping of nickel in ZnO nano-particles because the Ni doping has exhibited a drastic and interesting change in the optical, electrical, and magnetic properties.

Furthermore, Ni^{2+} (0.69\AA) has the same valence compared to Zn^{2+} and its radius is close to Zn^{2+} (0.74\AA), so it is very easy for Ni^{2+} sub-lattice to replace Zn^{2+} in ZnO lattice. Some researches on Ni doped ZnO have been reported and several results showed that the various properties of ZnO were changed after inserting Ni into ZnO matrix [12,13]. By doping Ni into ZnO, a composite material with magnetic and optical properties could be obtained. Magnetic material could be used in magnetic therapy and fluorescence material could be applied in phototherapy agents, so the Ni-doped ZnO would be a new material in medical field. The transition metal doped nanostructure is an effective method to adjust the energy levels and surface states of ZnO, which can further introduce changes in its physical and especially optical properties [14]. In addition to the UV excitonic emission peak, ZnO commonly exhibits the visible luminescence at different emission wavelengths due to the intrinsic or extrinsic defects [15]. Until now, zinc oxide with various shapes was prepared by various methods [16-25]. Out of these methods of ZnO synthesis, we have used a sol-gel chemical synthesis to prepare the nano-particles. However, it is still a great challenge to synthesize ZnO nano-

structures doped with the transition metal element using a simple process with a low cost. The solution growth method is an effective approach and has been a very promising route for synthesizing ZnO nano-materials at a low temperature. Therefore, the solution growth “sol-gel chemical method” is used to prepare undoped ZnO and Ni-doped nano-particles at a low temperature in this paper. The high quality nano-crystalline powders of $Zn_{1-x}Ni_xO$ ($x = 0.00, 0.01, 0.03$ and 0.05) are successfully synthesized and their structural and optical absorption and compositional properties are investigated. The present synthesis method is reproducible and ensures the large scale production at a low temperature.

2. Experimental Details

2.1. Synthesis Process

The Chemicals used in the synthesis processes are: Zinc acetate (ZA) ($Zn(CH_3COO)_2 \cdot 6H_2O$), Nickel Nitrate (NN) ($Ni(NO_3)_2 \cdot 6H_2O$), Ethylene Glycol (EG) ($CH_2(OH)CH_2OH$), Citric Acid (CA) ($C_6H_8O_4$) Ammonia solution (AS) (NH_3), Ethanol (ET) (CH_3CH_2OH) and Distilled water (DW) (H_2O).

Ni doped ZnO was synthesized by a simple dissolution followed by precipitation method. Starting materials used in this experiment were ZA for undoped and NN was mixed at mol.% for doped ZnO and CA used as a fuel. All the reagents were of analytical grade. The reaction was done at low pH value (i.e. 2.5); such reduction of pH was done by using CA. According to the appropriate proportion, the ZA (1.00, 0.99, 0.97 and 0.95) and NN (0.00, 0.01, 0.03 and 0.05) are completely dissolved in a beaker with 100 ml DW and stirred for an hour to get a homogenous solution. Then 10 ml EG was mixed for being strong bonding between compounds. In last the AS was added drop wise for precipitation, these all above steps was done at the temperature $70^\circ C$ on magnetic stirrer. The precipitated solution was filtered and cleaned with DW and ET several times to remove impurities and then dried at $120^\circ C$ for 6 hours in oven. To obtain Ni doped ZnO powder, the precipitate was heated in air atmosphere at $450^\circ C$ for 4 hours. The above procedure was also used to synthesize Mn-ZnO powder [26]. Finally, a reticular substance is obtained and then ground to powders in an agate mortar for an hour and used for further characterization studies. All the samples with different percentages of Ni doping ($Zn_{1-x}Ni_xO$) were prepared under identical conditions.

2.2. Characterization

The calcined nano-powders were characterized for crystal phase identification by X-ray diffraction (XRD) technique in the 2θ range of 20 – 80 (Rigaku Miniflex II) with $Cu K\alpha$ radiations ($\lambda = 1.5418 \text{ \AA}$) operated at voltage of 30 kV and current of 15 mA . SEM equipped with EDS measurement has been done by JEOL JSM-6510LV. UV-visible spectroscopy of undoped and Ni-ZnO NPs were performed in the range 350 – 700 nm using Perkin Elmer Spectrophotometer followed by the FT-IR techniques has been used for compositional analysis (finger print of the material).

3. Results and Discussion

3.1. Structural Determination

3.1.1. XRD Analysis

The crystal structure and phase purity of prepared undoped ZnO and different composition of Ni-doped ZnO nano-particles annealed at $450^\circ C$ were characterized using X-ray diffraction. Figure 1 shows a typical XRD spectra of pure ZnO and $Zn_{1-x}Ni_xO$ ($x = 0.00, 0.01, 0.03, 0.05$) nano-particles. XRD pattern reveals that the diffraction peaks of undoped and nickel doped ZnO nano-particles can be indexed to hexagonal wurtzite structure of ZnO which is in good agreement with the standard JCPDS file for ZnO (JCPDS36-1451, $a = 0.3279 \text{ nm}$, $c = 0.5204 \text{ nm}$ having space group $P63mc$). In all doped samples, the nickel traces were observed at (200) plane. This new phase emerges at ($2\theta = 42.5^\circ$) as shown in Figure 1. Such an additional diffraction peak corresponds to the secondary phase of NiO (200) (matched with JCPDS 78-0643). The intensity of NiO peak increases with increasing nickel amount (Figure 1 Inset) indicating that phase segregation has occurred and such structural degradation in the ZnO lattice may be attributed to introduction of a foreign impurity [27].

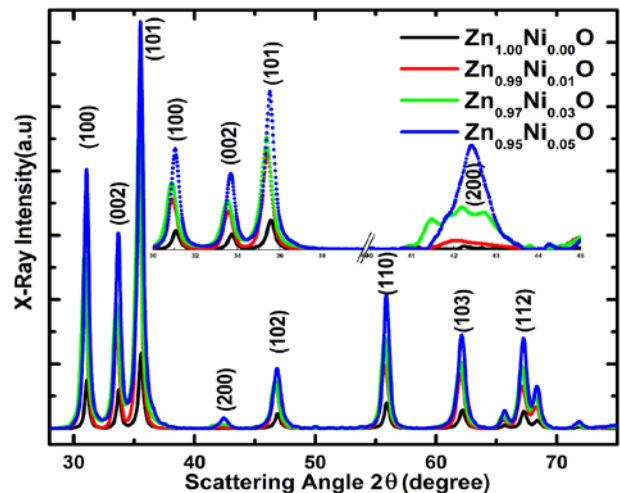


Figure 1. XRD spectra of Undoped and Ni-doped ZnO

The crystallite size may be calculated using Scherrer's formula;

$$D = \frac{k\lambda}{\beta \cos \theta}$$

Where λ is the wavelength of the X-rays, θ is the diffraction angle, D is the crystallite size, k is the shape factor (i.e. 0.94 for Lorentzian line profiles and small crystals of uniform size), β is the full width at half maximum (FWHM) of the peak. The calculated parameters are shown in Table 1.

The expansion of the lattice constants of Ni-doped ZnO nano-particles (Table 1) indicated that Ni ions systematically substituted into the ZnO matrices [28]. Morphology of the undoped ZnO nano-particles have been investigated using scanning electron microscopy (SEM), as shown in Figure 2. The spectrograph of the sample shows the growth of undoped ZnO nano-particles. It

indicates that the growth is not exactly in uniform grain size but in average it is observed like hexagonal nanostructure. Figure 3 shows the EDS spectra which has

confirmed that the synthesized sample contain only Zn and O without any impurity phase rather carbon which is due to the carbon tape used at the time of EDS analysis.

Table 1. Calculated parameters of undoped and Ni doped ZnO Nano-particles

Ni Conc. (%)	FWHM (rad)	D(nm)	E_g (eV)	Lattice parameter (Å)			Unit Cell Vol.(Å ³)
				a	b	c	
0	0.4600	18.12	3.01	3.279	3.279	5.204	55.95
1	0.4400	18.95	2.90	3.300	3.300	5.270	57.39
3	0.4300	19.39	2.60	3.302	3.302	5.271	57.47
5	0.5646	14.77	3.16	3.270	3.270	5.200	55.60

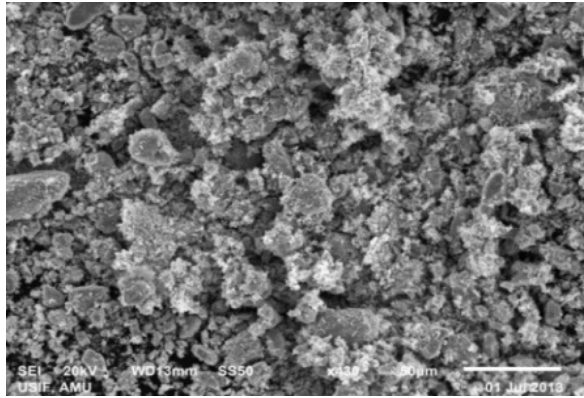


Figure 2. SEM micrograph of undoped ZnO

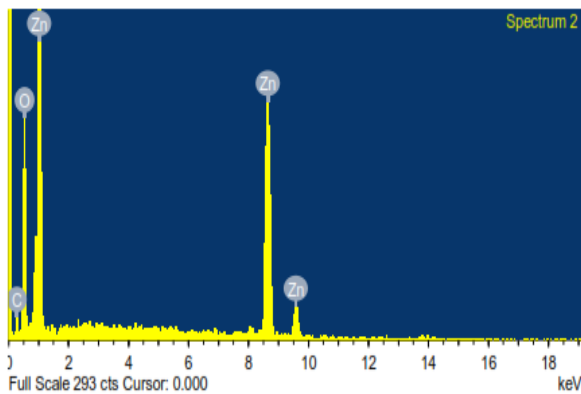


Figure 3. EDS spectra of undoped ZnO

3.1.2. Compositional Analysis

The formation of the wurtzite ZnO structure in undoped and doped ZnO nanocrystalline powders is further confirmed by FTIR spectra as shown in Figure 4. The FTIR spectra were recorded in the range of 400–4000 cm^{-1} for all samples. The position and number of absorption bands not only depend on crystal structure and chemical composition but also on crystal morphology. The peaks around 1336 and 1537 cm^{-1} are attributed to the symmetric and asymmetric C=O stretching vibration modes, while the peak at 441 cm^{-1} is attributed to the stretching E2 (LO) mode which is typical for the ZnO wurtzite structure. In Figure 4, appearance of small peak at 1000 cm^{-1} is attributed to C-H stretching. A small hump observed at 1900–2051 cm^{-1} revealed the presence of O-C-O which appeared due to the atmospheric absorption at the preparation time of sample in non-vacuum system. A strong absorption peaks in all undoped and Ni-ZnO samples have been observed at 3331 cm^{-1} which is attributed to the presence of hydroxyl group (O-H stretching). It is important to notice that the doping specie affects the spectra and it has been observed that the

broadening at the shoulder of ZnO band at 480 cm^{-1} attached to the ZnO peaks which assigned as Ni-O stretching mode, which is be due to the Ni ion present in the doped samples. Hence, it is nice supporting result of previous investigations in this paper.

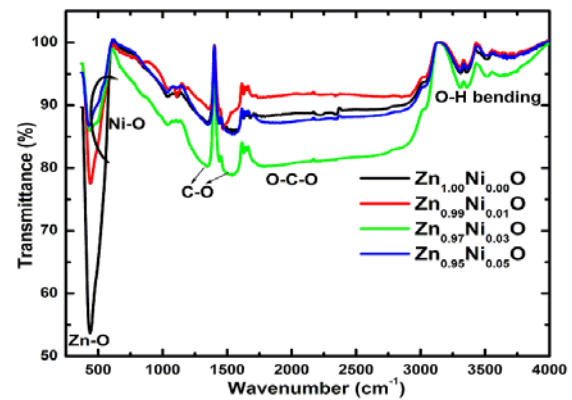


Figure 4. FTIR spectra on undoped and Ni-doped ZnO

3.2. Optical Properties

The effect of Ni substitution on wurtzite structure of ZnO was further confirmed using UV–visible optical spectroscopy measured in the range 300–800 nm. Figure 5 shows the room temperature optical absorption spectra of undoped and nickel doped ZnO nano-particles. The absorption band edge of undoped ZnO is observed at 373 nm and it gets shifted towards longer wavelength region for the 1 and 3 mol. % Ni-doped ZnO samples and goes to lower wavelength for 5 mol.%. The observed red shift in the absorption band edge with nickel doping in ZnO may be due to the *sp-d* exchange interactions between the band electrons and the localized *d*-electrons of the Ni^{2+} ions. Such a red shift in band edge with increasing nickel dopant is a clear indication for the incorporation of Ni ions into the Zn site of the ZnO matrix [26,27,28].

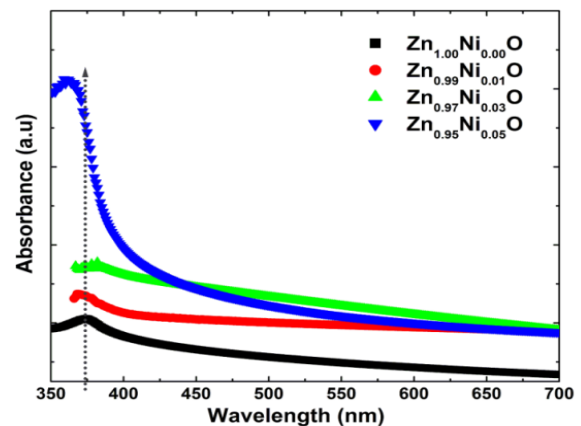


Figure 5. Absorbance spectra of undoped and Ni-doped ZnO

It may be noted that the band gap of pure NiO is in the range of 3.5- 4.0 eV. So the doping is not tuning of the band gap in the direction of NiO at lower doping amount. Perhaps, it is not surprising that the band gap upon doping is a consequence of the interaction between Ni and ZnO states. This band gap reduction at lower percentage of Ni could be attributed to the introduction of Ni states which lowers the valance band states. Instead, at higher % of Ni substitution there is increased the NiO sublattice like phase which may not adhered to the ZnO lattice, therefore, NiO sublattice is dominating for the higher band gap occurrence. Otherwise, the quantum confinement effect is

directly showing the variation of band gap with the crystallite size.

The absorption coefficient and the energy band gap can be described by the following equation;

$$\alpha h\nu = B(h\nu - E_g)^{1/2}$$

where $h\nu$ is the photon energy, α is the absorption coefficient, and B is a constant.

A plot of $(\alpha h\nu)^2$ versus $h\nu$ is made to determine bandgap E_g using the linear fit process. The extrapolated absorption threshold of the undoped and Ni-doped ZnO nano-particles is shown in Figure 6.

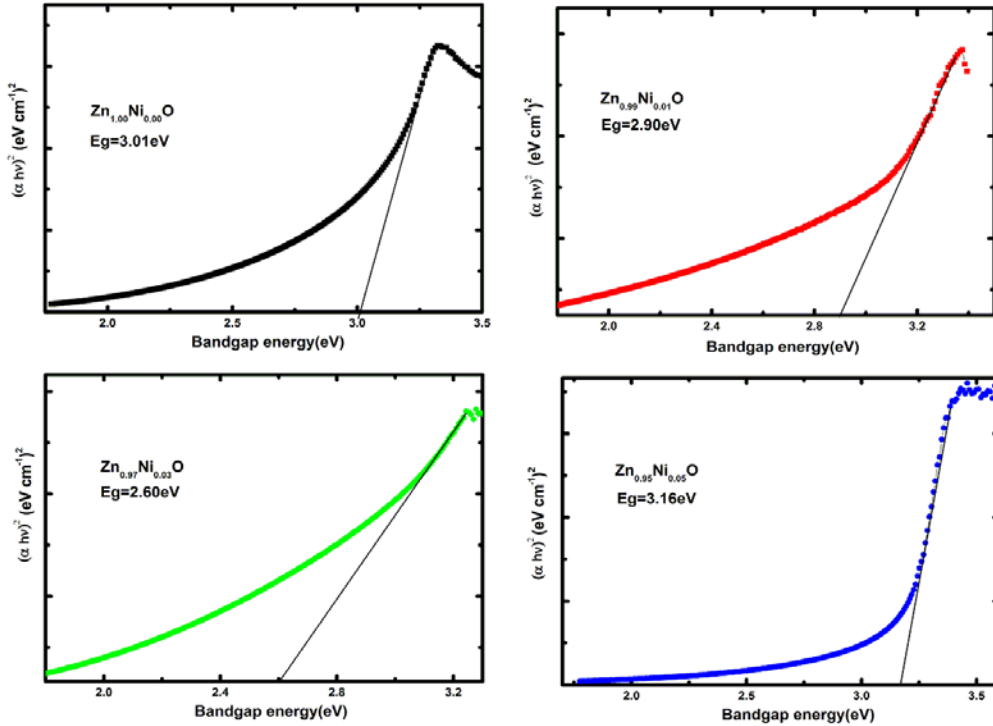


Figure 6. Band gap spectra of undoped and Ni ZnO NPs

It reflects the band gap energies of the corresponding samples and indicates that the bandgap decreases with 1 and 3 mol % nickel doping and further doping at 5 mol. % band gap goes to the higher value. The bandgap decreasing with increasing nickel dopant could be interpreted mainly due to the $sp-d$ exchange interactions between the band electrons and the localized d electrons of the Ni^{2+} ions. Quantum mechanically, we can interpret the absorption falls at higher percentage of Ni which results in the bandgap broaden. It is due to the fact that as the crystallite decreasing in size to low dimension as enough, the quantum confinement effect came in existence which enhances the band gap [29]. Therefore, the energy bandgap linearly depends on $1/D^2$ as shown in Figure 7. In the strong confinement regime, the confinement energy of the first excited electronic state can be approximated by the following equation [30];

$$E_{(bandgap)} = E_{(undoped)} + \frac{2\pi^2\hbar^2}{D^2} \left(\frac{1}{m_e^*m_0} + \frac{1}{m_h^*m_0} \right) - 0.248E_{ex}^*$$

where the undoped bandgap $E_{undoped}$ is 3.01eV (this work) and the bulk exciton binding energy E_{ex}^* can be

taken as 60 meV. According to Beni and Rice [31] the electron and hole effective masses are taken as $m_e^* = 0.24m_0$ and $m_h^* = 2.31m_0$, respectively. Additionally, \hbar is the reduced Planck's constant and D is crystallite size calculated from XRD measurements.

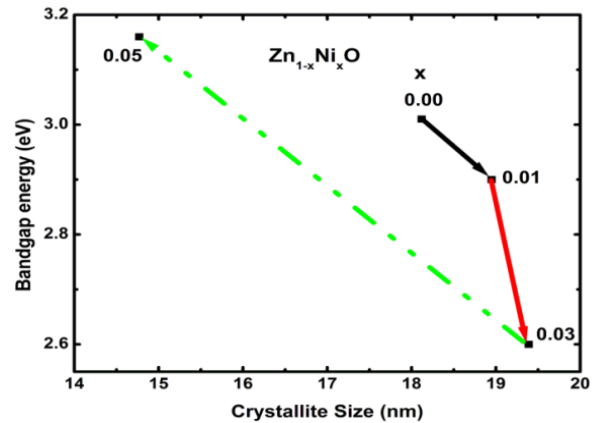


Figure 7. Energy bandgap variation with crystallite size

From above equation, we can interpret that the variation of band gap for Ni doped ZnO is $1/D^2$ dependent as shown in Figure 7, which is nothing but only due to the quantum confinement effect. Thus, Ni ions exist in a tetrahedral

crystal field in the +2 state without changing the wurtzite crystal structure of ZnO.

4. Conclusions

We have synthesized a series of undoped and nickel (Ni) doped ZnO Nano-particles using sol-gel method with citric acid as the fuel. The crystal structure of the $Zn_{1-x}Ni_xO$ compound with $x=0.00, 0.01, 0.03$ and 0.05 has been studied. From XRD data, it is confirmed that all samples are in the wurtzite hexagonal structure. No secondary phases have been observed in the present work for the Ni-ZnO samples and it is to be reported that the doping effect of Ni present at (200) plane. The crystallite size was found to be increase up to the 3% doping and then decreased for heavy doping which results in bandgap decreases and increases respectively. This can be attributed to the quantum confinement effect and it has been observed that the band gap linearly depends on $1/D^2$. The FTIR spectroscopy has been done for complete structural analysis for all the samples which assigned prominent peaks for different species and it is confirmed that the Zn-O, C-C, C-O-O bands as major and hydroxyl group as a minor component presents in powders. Henceforth, we infer that all the above studies have been analyzed for nickel sub-lattice effects on ZnO which may provide the fundamental understanding for many application purposes.

Acknowledgement

Authors are highly grateful to the Centre of Excellence in Materials Science (Nano-materials) Department of Applied Physics, Faculty of Engineering and Technology, Aligarh Muslim University, Aligarh for providing us the experimental facilities. We are deeply acknowledged to the Department of physics, Aligarh Muslim University, Aligarh for their valuable financial support for this work under DIST-FIST programme.

References

- [1] Miyake A, Kominami H, Tatsuoka H, Kuwabara H, Nakaushi Y and Hatanaka Y, 2000, Luminescent properties of ZnO thin films grown epitaxially on Si substrate, *J. Cryst. Growth* pp. 214-215, 294.
- [2] Song D, Aberle A G and Xia J, 2002, Optimization of ZnO: Al films by change of sputter gas pressure for solar cell application, *Appl. Surf. Sci.* 195, 291.
- [3] Martinez M A, Herrero J and Gutiérrez M T, 1997, Deposition of transparent and conducting Al-doped ZnO thin films for photovoltaic solar cells, *Sol. Energy Mater. Sol. Cells* 45, 75.
- [4] Cheng X L, Zhao H, Huo L H, Gao S and Zhao J G, 2004, ZnO nano-particulate the films: preparation characterization and gas-sensing property, *Sensors Actuators B* 102, 248.
- [5] Ko S C, Kim Y C, Lee S S, Choi S H and Kim S R, 2003, micro-machined Piezoelectric Membrane acoustic device, *Sensors Actuators A* 103, 130.
- [6] Kang H S, Kang J S, Kim J Wand Lee S Y, 2004, Annealing effect on the property of ultraviolet and green emission of ZnO thin films, *J. Appl. Phys* 95, 1246.
- [7] Major S and Chopra K L, 1988, indium doped zinc oxide films as transparent electrodes for solar cells, *Sol. Energy Mater.* 17, 319.
- [8] S. J. Pearton, D.P. Norton, K. Ip, Y.W. Heo, T. Steiner, 2003, Recent progress in processing and properties of ZnO, *Superlattices and Microstructures*, 34, 3-32.
- [9] J. Zhou, N.S. Xu, Z.L. Wang, 2006, Dissolving behavior and stability of ZnO Wires in bio fluids: a study on biodegradability and biocompatibility of ZnO nanostructures, *Adv. Mater.* 18, 2432-2435.
- [10] K. Sato, H. Katayama-Yoshida, 2000, Material design for transparent ferromagnets with ZnO-based magnetic semiconductors, *J. Appl. Phys.* 39, 555-558.
- [11] A. Korbecka, J.A. Majewski, 2009, on the origin of room-temperature ferromagnetism in wide-gap semiconductors, *Low Temp. Phys.* 35, 53-57.
- [12] D. Karmakar, S.K. Mandal, R.M. Kadam, P.L. Paulose, A.K. Rajarajan, T.K. Nath, A.K. Das, I. Dasgupta, G.P. Das, 2007, Ferromagnetism in Fe-doped ZnO nanocrystals: experiment and theory, *Phys. Rev. B* 75, 144404.
- [13] C.W. Cheng, G.Y. Xu, H.Q. Zhang, Y. Luo, 2008, Hydrothermal synthesis Ni-doped ZnO nanorods with room-temperature ferromagnetism, *Material Letters*, 62, 1617-1620.
- [14] D.W.Wu, M. Yang, Z.B. Huang, G.F. Yin, X.M. Liao, Y.Q. Kang, X.F. Chen, H. Wang, 2009, Preparation and properties of Ni-doped ZnO rod arrays from aqueous solution, *J. Colloid Interface Sci.* 330, 380-385.
- [15] M. Sima, I. Enculescu, M. Sima, M. Enache, E. Vasile and J. P. Ansermet, 2007, ZnO:Mn:Cu nanowires prepared by template method, *Phys. Status Solidi B* 244, 1522.
- [16] A. B. Djurišić, W. C. H. Choy, V. A. L. Roy, Y. H. Leung, C. Y. Kwong, K. W. Cheah, T. K. Gundu Rao, W. K. Chan, H. F. Lui and C. Surya, 2004, Photoluminescence and EPR of ZnO tetrapod structures, *Adv. Funct. Mater.* 14, 856.
- [17] L.P. Bauermann, A. Campo, J. Bill, F. Aldinger, 2006, Heterogeneous nucleation of ZnO using gelatin as the organic matrix, *Chem. Mater.* 18, 2016-2020.
- [18] M. Umetsu, M. Mizuta, K. Tsumoto, Satoshi Ohara, S. Takami, H. Watanabe, I. Kumagai, T. Adschiri, 2005, Bio assisted room-temperature immobilization and mineralization of zinc oxide—the structural ordering of ZnO nano-particles into a flower-type morphology, *Adv. Mater.* 17, 2571-2575.
- [19] M.S. El-shall, W. Slack, W. Vann, D. Kane, D. Hanley, 1994, Synthesis of nanoscale metal oxide particles using laser vaporization/condensation in a diffusion cloud chamber, *J. Phys. Chem.* 98 (12), 3067-3070.
- [20] X.F. Duan, C.M. Lieber, 2000, General synthesis of semiconductor nanowires, *Adv. Mater.* 12 (4), 295-302.
- [21] J.T. Hu, T.W. Odom, C.M. Lieber, 1999, Chemistry and physics in one dimension: synthesis and properties of nanowires and nanotubes, *Acc. Chem. Res.* 32 (5), 435-445.
- [22] Y.N. Xia, P.D. Yang, Y.G. Sun, Y.Y. Wu, B. Mayers, B. Gates, Y.D. Yin, F. Kim, H.Q. Yan, 2003, One-dimensional nanostructures: synthesis, characterization, and applications, *Adv. Mater.* 15 (5), 353-359.
- [23] S.S. Fan, M.G. Chapline, N.R. Franklin, T.W. Tombler, A.M. Cassell, H.J. Dai, 1999, Self-oriented regular arrays of carbon nanotubes and their field emission properties, *Science* 2839 (2), 512-514.
- [24] M.H. Huang, S. Mao, H. Feick, H.Q. Yan, Y.Y. Wu, H. Kind, E. Weber, R. Russo, P.D. Yang, 2001, Room-temperature ultraviolet nanowire and nanolasers, *Science* 2929 (29), 1897-1899.
- [25] M. Li, H. Schnablegger, S. Mann, 1999, Coupled synthesis and self-assembly of nanoparticles to give structures with controlled organization, *Nature* 402 (5), 393-395.
- [26] M. Mo, J.C. Yu, L. Zhang, S.A. Li, 2005, Self-assembly of ZnO nanorods and nanosheets into hollow micro hemispheres and microspheres, *Adv. Mater.* 17 (6), 756-760.
- [27] Sajid Husain, F. Rahman, Wasi Khan, and A. H. Naqvi, Effects of Mn substitution on Structural And Optical Properties of ZnO Nanoparticles, 2013, *AIP Conf. Proc.* 1536, 33.
- [28] P.K. Sharma, R.K. Dutta, A.C. Pandey, 2009, Effect of nickel doping concentration on structural and magnetic properties of ultrafine diluted magnetic semiconductor ZnO nanoparticles, *J. Magn. & Magn. Mater.* 321, 3457.
- [29] G.J. Huang, J.B. Wang, X.L. Zhong, G.C. Zhou, H.L. Yan, 2007, Synthesis, structure, and room-temperature ferromagnetism of Ni-doped ZnO nano-particles, *J. Mater. Sci.* 42, 6464.
- [30] A.L. Efros and M. Rosen, 1998, Quantum size level structure of narrow-gap semiconductor nanocrystals: Effect of band coupling, *Physical Rev. B*, 58, 7120.
- [31] G. Beni and T. M. Rice, 1978, Theory of electron-hole liquid in semiconductor, *Phys. Rev. B* 18, 768.